

Synthetic and Structural Studies of 1-Halo-8-(alkylchalcogeno)naphthalene Derivatives

Fergus R. Knight, Amy L. Fuller, Michael Bühl, Alexandra M. Z. Slawin, and J. Derek Woollins*^[a]

Abstract: A series of eight 1-halo-8-(alkylchalcogeno)naphthalene derivatives (**1–8**; halogen = Br, I; alkylchalcogen = SEt, SPh, SePh, TePh) containing a halogen and a chalcogen atom occupying the *peri* positions have been prepared and fully characterised by using X-ray crystallography, multinuclear NMR spectroscopy, IR spectroscopy and MS. Naphthalene distortion due to non-covalent substituent interactions was studied as a function of the bulk of the interacting chalcogen atoms and the size and nature of the alkyl group

attached to them. X-ray data for **1**, **2**, **4** and **5–8** were compared. Molecular structures were analysed in terms of naphthalene ring torsions, *peri*-atom displacement, splay angle magnitude, X...E interactions, aromatic ring orientations and quasi-linear X...E–C arrangements. A general increase in the

Keywords: chalcogens • density functional calculations • halogens • naphthalene • *peri*-substitution • X-ray diffraction

X...E distance was observed for molecules that contain bulkier atoms at the *peri* positions. The I...S distance of **4** is comparable with the I...Te distance of **8**, and is ascribed to a stronger lone pair–lone pair repulsion due to the presence of an axial S(naphthyl) ring conformation. Density functional theory (B3LYP) calculations performed on **5–8** revealed Wiberg bond index values of 0.05–0.08, which indicate minor interactions taking place between the non-bonded atoms in these compounds.

Introduction

Sterically overcrowded systems incorporating bulky heteroatoms at distances shorter than the sum of their van der Waals (vdW) radii have attracted great attention over the last decade.^[1] When heteroatoms are confined to unavoidably cramped environments, they suffer steric hindrance that gives rise to structurally distorted compounds with unusual bonding and geometry. The potential for weak non-covalent interactions to occur between tightly packed heteroatoms is of particular importance. Atomic interactions are a fundamental aspect of chemistry, biology and materials science.^[2] Although great advances have been made in the area of

strong covalent and ionic bonding, a major challenge for chemists is to develop a full understanding of weak intra- and intermolecular forces.

The field of *peri*-substituted naphthalenes has received a large amount of attention and has developed to encompass topics such as hypercoordination, hypervalency and three-centre–four-electron (3c–4e) interactions.^[1] *Peri*-substituted naphthalenes are able to constrain heavy polarisable elements in close proximity owing to their rigid C₂ backbone and are, therefore, ideal models for studying such systems. The distance between the *peri*-carbon atoms in “ideal” naphthalene (2.44 Å),^[3] can adequately support two hydrogen atoms, but larger substituents will experience considerable steric hindrance.^[4] Repulsive steric effects caused by the crowding of substituents can be overcome by attractive, weak or strong intramolecular bonding, or by distortion of the naphthalene skeleton away from ideal.^[4,5] The most common forms of naphthalene distortions are in-plane and out-of-plane deviations of the exocyclic bonds and buckling of the naphthalene ring system.^[4]

The availability of X-ray structural data plays a crucial role in assessing the repulsive steric effects between heavy *peri* substituents and thus quantifying the distortion in non-ideal naphthalenes.^[5] Molecular structures also help to eluci-

[a] F. R. Knight, Dr. A. L. Fuller, Dr. M. Bühl, Prof. A. M. Z. Slawin, Prof. J. D. Woollins
School of Chemistry
University of St Andrews
St Andrews, Fife
KY16 9ST (UK)
Fax: (+44) 1334-463384
E-mail: jdw3@st-and.ac.uk

Supporting information for this article is available on the WWW under <http://dx.doi.org/10.1002/chem.201000435>, and contains X-ray crystallographic data for **2**, **4** and **6–8**.

date attractive effects between *peri* atoms and verify the existence of weak intra- and intermolecular interactions. To quantify the extent of naphthalene distortion taking place in a given molecule, the naphthalene geometry is compared with that of ideal, or un-substituted, naphthalene.^[3] In-plane distortion is calculated by observing the sum of angles in the bay region; in the ideal geometry of naphthalene these angles sum to 357.2°.^[3] If the splay angle (sum of the bay region angles > 360) is positive we can conclude the bonds have moved apart, which indicates steric repulsion, but negative splay angles may suggest that the atoms have come closer together as a result of favourable interactions.^[3,6,7]

The distance the *peri* substituents reside above and below the naphthalene plane measures out-of-plane distortion; in ideal naphthalene the *peri* hydrogens lie on the naphthyl plane.^[3] Lastly, torsion angles indicate the planarity of the molecule and give an insight into the degree of buckling taking place in the naphthalene ring system. Ideal naphthalene is totally planar, with torsion angles of either 0 or 180°.^[3,6] The three types of distortion are cumulatively expressed by the value of the *peri* distance, which is used as the primary parameter when describing the distortion away from ideal and also to indicate the presence of *peri*-atom interactions.^[6]

Attractive interatomic interactions acting between chalcogen lone pairs have received some attention.^[8] Current research in this area utilises the rigid C₃ naphthalene backbone to constrain Group 16 elements in close proximity, which results in a substantial overlap of orbitals. Nakanishi et al.^[2,8–12] studied organo-selenium compounds that show typical examples of chalcogen lone pair-lone pair interactions. At the start of their project they synthesised bis[8-(phenylselanyl)naphthyl]-1,1'-diselenide **A** and 1-(methylselanyl)-8-(phenylselanyl)naphthalene **B** (Figure 1).^[1h,9] From X-ray crystallography, the molecular structure of **A** revealed a quasi-linear arrangement of four selenium atoms. To help rationalize both structures, ab initio MO calculations were performed. The linear arrangement in **A** was reported to arise as the result of an energy-lowering effect due to the construction of a four-centre-six-electron (4c–6e) bond,^[1h,9] whereas the lone-pair interaction taking place in **B** suggested a two-centre-four-electron (2c–4e) interaction.^[1h,9]

In a subsequent paper, Nakanishi et al. prepared 8-fluoro-1-(*p*-anisylselanyl)naphthalene **C** (Figure 1).^[10] The molecular structure exhibits a linear alignment of the type F··Se–C with an F–Se–C angle of 175.0°. Following ab initio MO calculations, the linear arrangement was found to result from a charge transfer from the fluorine atom to the σ* orbital of selenium.^[10]

Expanding their research, Nakanishi et al. went on to study the effects of nonbonded G··Se–C 3c–4e interactions on the structures of a series of compounds with the 8-G-1-(*p*-YC₆H₄Se)C₁₀H₆ structural motif. Compounds **D–G** (see Figure 1) were synthesised^[2,8–12] and X-ray crystal structures were obtained for **D****b–d**, **E****d,g**, **H****a,b,d** and **G****a–f**. Each structure was classified as type A, B or C depending upon

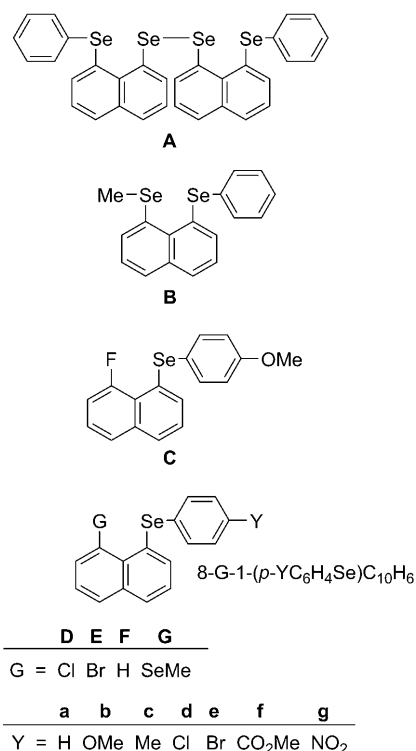


Figure 1. Compounds investigated by Nakanishi et al.^[2,8–12]

the position of the Se–C_{Ar} bond relative to the mean naphthalene plane (in type A the Se–C_{Ar} bond lies almost perpendicular to the naphthalene plane, in type B the bond is located on the plane and in type C the structure is intermediate between types A and B).^[1h,2,8,9,11]

The structures of the members of **D**, **E**, **F** and **G** that were not determined by X-ray crystallographic analysis were estimated from ab initio MO calculations and NMR studies.^[2,8–12] Nakanishi et al. found that compounds in which G = Cl or Br always adopt the type B structure irrespective of the group that occupies the Y position; these compounds thus contain the linear non-bonded G··Se–C arrangement. On the basis of ab initio MO calculations they concluded that the linear alignment of the three atoms must be the result of the non-bonded G··Se–C 3c–4e type interaction.^[8]

We have previously explored sterically crowded 1,8-disubstituted naphthalenes.^[6,13,14] Our early work focussed on dichalcogenide ligands^[13] and unusual phosphorus compounds,^[6,14] but we have recently been studying mixed phosphorus–chalcogen^[15] and chalcogen–chalcogen systems.^[16] Positioning large elements, such as those of Group 16 or 17, in close proximity at the 1,8-positions in naphthalene causes steric compression and provides good systems with which to study naphthalene distortion and the emergence of non-covalent *peri*-atom interactions.

The work presented herein complements our earlier studies of chalcogen-based systems^[16] and the work undertaken by Nakanishi et al. on 8-G-1-(*p*-YC₆H₄Se)C₁₀H₆-type compounds.^[8] Herein we report the synthesis and structural analysis of two compounds that adopt this structural motif,

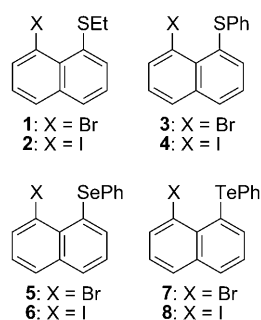


Figure 2. The products of single substitution reactions of 1,8-dibromo- and 1,8-diiodonaphthalene with diethyl or diphenyl dichalcogenides.

along with six analogous (sulfur and tellurium) mixed halogen–chalcogen *peri*-substituted systems **1–8** (Figure 2). Compounds **1–8** were prepared through a new synthetic route by using halogen–lithium exchange reactions of 1,8-dibromonaphthalene **9** and 1,8-diiodonaphthalene **10**, although **1**,^[17,18] **3**^[19,20] and **5**^[8,20,21] have been previously reported; compound **5** was previously reported by Nakanishi et al. and in the same study the chloro analogue **Da** was synthesised.^[8]

From ab initio MO calculations,

the chloro and fluoro derivatives were estimated to adopt a similar structure to that of **5** (type B).^[8] To the best of our knowledge, the chloro and fluoro analogues of the SEt, SPh and TePh derivatives are unknown.

Herein, molecular structures of **1**, **2** and **4–8** (determined by X-ray crystallography) are compared in terms of molecular distortion in the naphthalene scaffold and the geometry around the chalcogen atom. For each structure, naphthalene ring torsion angles, *peri*-atom displacement, splay angle magnitude, X⋯E interactions, aromatic ring orientations and quasi-linear C–E⋯X arrangements were calculated. We have previously published the structures of **1**^[18] and **5**.^[21] The structural conformations of **1**, **2** and **4–8** have been characterised based on the classification system proposed by Nakanishi et al.^[1h,2,8,9,11]

Results and Discussion

Compounds **1–8** were synthesised and crystal structures were determined for **1**, **2** and **4–8**. Except for previously reported compounds **1**^[17] and **5**,^[8] all derivatives were spectrally characterised by using multinuclear NMR and IR spectroscopies and mass spectrometry and the homogeneity of the new compounds was confirmed by microanalysis where possible.

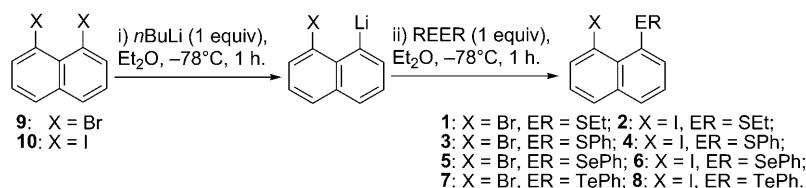
The series of 1-halo-8-(alkylchalcogeno)naphthalene derivatives (**1–8**) was prepared with a new synthetic route by using the stepwise halogen–lithium exchange reactions of analogous 1,8-dibromonaphthalene **9**^[22] and 1,8-diiodonaphthalene **10**,^[23] as shown in Scheme 1. For the synthesis of **1–**

8, compounds **9** and **10** were independently treated with a single equivalent of *n*-butyllithium in diethyl ether, which substituted one of the halogen atoms to afford the respective 1-halo-8-lithionaphthalene precursor. The addition of a suitable dichalcogenide (diethyl disulfide, diphenyl disulfide, diphenyl diselenide or diphenyl ditelluride) to the reaction mixture consequently afforded compounds **1–8** (yield: 43 (**1**), 42 (**2**), 51 (**3**), 26 (**4**), 63 (**5**), 60 (**6**), 32 (**7**) and 18% (**8**); Scheme 1).

Compounds **1–8** were characterised by using elemental analysis, IR spectroscopy, ¹H and ¹³C NMR spectroscopy and mass spectrometry. Compounds **5** and **6** were analysed by using ⁷⁷Se NMR spectroscopy (**5**: δ = 447.8 ppm; **6**: δ = 430.8 ppm) and **7** and **8** were analysed by using ¹²⁵Te NMR spectroscopy (**7**: δ = 731.23 ppm; **8**: δ = 698.26 ppm). Characterisation data for **1** and **5** were found to be in accord with the literature.^[8,17]

X-ray investigations: Single crystals of **1**, **2** and **4–8** suitable for X-ray diffraction were obtained by diffusion of pentane into saturated solutions of each individual compound in dichloromethane. Compound **3** was found to occur as an oil at room temperature. The molecular structures of **1**, **2** and **4–8** are analysed together here, although **1**^[18] and **5**^[21] have been previously reported by us. Compounds **2** and **4–8** crystallise with one molecule in the asymmetric unit whereas compound **1** contains two nearly identical molecules in the asymmetric unit. Figure 3 shows the structures of **2**, **4**, **6** and **7–8** respectively. Selected interatomic distances, angles and torsion angles are listed in Table 1. Further crystallographic information can be found in Table 4 and the Supporting Information.

The substitution of large halogen and chalcogen atoms in the 1,8-positions of derivatives **1–8** imposes a great amount of steric strain between the *peri* atoms. The subsequent displacement of the *peri* atoms within and away from the naphthalene plane is accompanied by a significant buckling of the naturally planar naphthalene skeleton and assists in alleviating the strain. The observed distortion correlates to the bulk of the two interacting atoms in the naphthalene molecule, as indicated by the *peri* distance, which is the primary parameter for naphthalene distortion. The structures of **1**, **2** and **4–8** reveal that the halogen atom lies in close proximity to the E(alkyl) group in all cases, with non-bonded interatomic *peri*-distances (X⋯E) displaying a general increase when larger atoms occupy the close contact 1,8-positions (see Table 1 and Figure 4). The X⋯E distances (3.06–3.34 Å) are less than the respective sum of the vdW radii for the two interacting atoms (3.65–4.04 Å),^[24] and in all derivatives this distance is between 82 and 88% of the vdW sum (Table 1).^[24] These short non-bonded *peri* distances indicate the possible existence of weak intramolecular interactions.^[25]



Scheme 1. The preparation of 1-halo-8-(alkylchalcogeno)naphthalenes **1–8**.

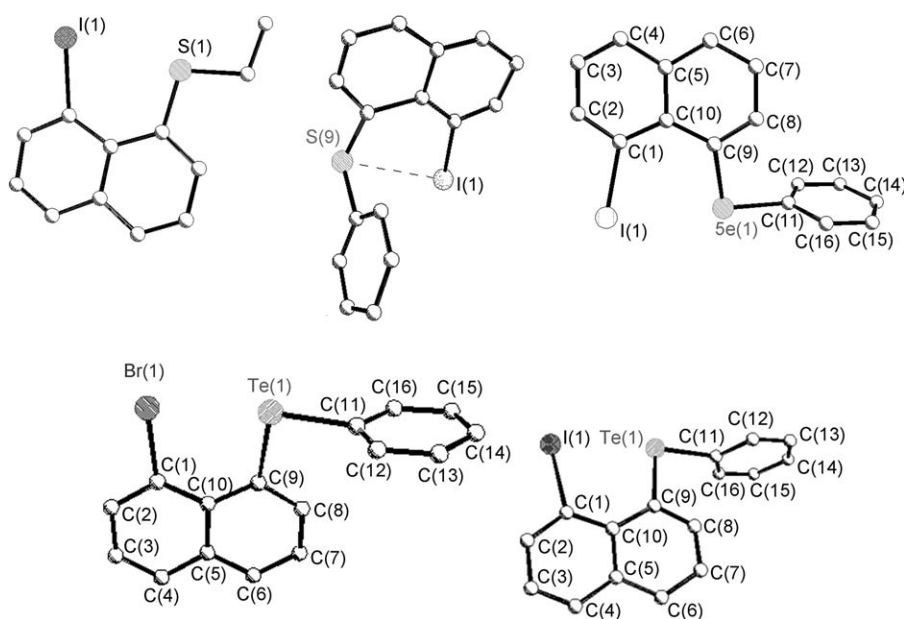


Figure 3. The crystal structures of 1-iodo-8-(ethylsulfanyl)naphthalene (**2**), 1-iodo-8-(phenylsulfanyl)naphthalene (**4**), 1-iodo-8-(phenylselenyl)naphthalene (**6**), 1-bromo-8-(phenyltelluro)naphthalene (**7**) and 1-iodo-8-(phenyltelluro)naphthalene (**8**).

Bond lengths around C(10), closer to the repulsive interactions, are on average longer than those around C(5) (average 1.44 and 1.42 Å, respectively) and C(1)–C(10)–C(9) bond angles splay to a mean 129° away from the ideal geometry as observed for C(4)–C(5)–C(6) (average 119°).^[3] The aforementioned bond stretching and angle widening distortions alone are insufficient to overcome the steric strain between the *peri* atoms. Supplementary widening of the E(1)–C(1)–C(10) and E(2)–C(9)–C(10) angles and displacement of the *peri* atoms from the mean naphthyl plane takes place to aid the alleviation of steric pressure.

The halogen and chalcogen atoms are displaced to different

Table 1. Selected interatomic distances [Å] and angles [°] for Nap[X][ER]compounds **1**, **2** and **4–8**.^[a]

	1 ^[18]	2	4	5 ^[21]	6	7	8
X, ER	Br, SEt	I, SEt	I, SPh	Br, SePh	I, SePh	Br, TePh	I, TePh
<i>peri</i> -Region distances							
X(1)⋯E(1)	3.0561(18) (3.0505(19))	3.2436(17)	3.338(11)	3.1136(6)	3.2524(8)	3.1909(10)	3.3146(6)
Σ _{r_{vdW}–X⋯E} ^[b]	0.5939 (0.5995)	0.5364	0.442	0.6364	0.6276	0.7191	0.7254
Σ _{r_{vdW}} ^[b] [%]	84 (84)	86	88	83	84	82	82
X(1)–C(1)	1.901(6) (1.897(6))	2.126(6)	2.118(11)	1.919(3)	2.122(4)	1.917(6)	2.108(6)
E(1)–C(9)	1.770(6) (1.778(6))	1.773(6)	1.765(11)	1.948(3)	1.958(4)	2.153(6)	2.151(6)
Naphthalene bond lengths							
C(1)–C(2)	1.365(9) (1.381(9))	1.384(9)	1.363(14)	1.363(6)	1.373(7)	1.382(12)	1.382(12)
C(2)–C(3)	1.403(10) (1.391(9))	1.391(10)	1.406(15)	1.402(5)	1.402(7)	1.387(11)	1.389(10)
C(3)–C(4)	1.348(9) (1.331(10))	1.343(9)	1.342(17)	1.354(5)	1.372(9)	1.352(10)	1.356(10)
C(4)–C(5)	1.395(9) (1.417(10))	1.409(9)	1.467(19)	1.436(6)	1.418(7)	1.417(12)	1.400(11)
C(5)–C(10)	1.446(8) (1.441(8))	1.435(8)	1.414(17)	1.433(5)	1.449(6)	1.440(9)	1.454(8)
C(5)–C(6)	1.443(9) (1.404(9))	1.409(9)	1.393(19)	1.420(5)	1.414(9)	1.422(9)	1.411(9)
C(6)–C(7)	1.312(9) (1.376(10))	1.348(11)	1.358(19)	1.373(6)	1.372(8)	1.399(13)	1.379(12)
C(7)–C(8)	1.398(8) (1.388(10))	1.410(11)	1.319(17)	1.395(5)	1.416(7)	1.363(10)	1.365(10)
C(8)–C(9)	1.371(9) (1.382(9))	1.387(10)	1.425(16)	1.384(5)	1.366(8)	1.384(9)	1.346(9)
C(9)–C(10)	1.443(8) (1.415(9))	1.449(9)	1.458(15)	1.434(6)	1.452(7)	1.433(11)	1.443(11)
C(10)–C(1)	1.419(8) (1.433(9))	1.439(9)	1.441(15)	1.431(5)	1.437(8)	1.419(9)	1.418(9)
<i>peri</i> -Region bond angles							
X(1)–C(1)–C(10)	124.5(4) (124.1(4))	127.1(4)	127.2(8)	122.1(3)	124.2(3)	121.7(6)	123.4(5)
C(1)–C(10)–C(9)	128.8(5) (128.1(5))	128.2(5)	128.4(10)	128.3(3)	128.3(4)	128.6(6)	129.2(5)
E(1)–C(9)–C(10)	121.2(4) (122.9(5))	121.6(4)	125.2(8)	122.6(2)	122.4(4)	123.3(4)	123.6(4)
Σ of bay angles	374.5(9) (375.1(9))	376.9(9)	380.8(18)	373.0(6)	374.9(7)	373.6(10)	376.2(9)
Splay angle ^[c]	14.5 (15.1)	16.9	20.8	13.0	14.9	13.6	16.2
C(4)–C(5)–C(6)	119.5(5) (118.9(5))	117.8(5)	117.0(12)	118.5(3)	118.8(4)	118.9(6)	118.9(6)
X(1)–E(1)–C(11)	169.7(1) (169.8(1))	167.3(1)	85.8(1)	175.7(1)	174.3(1)	173.1(1)	175.1(1)
Out-of-plane displacement							
X(1)	–0.14(1) (0.01(1))	0.36(1)	–0.072(1)	0.40(1)	0.50(1)	0.4058(84)	–0.4152(86)
E(1)	0.04(1) (–0.04(1))	–0.17(1)	0.049(1)	–0.42(1)	–0.42(1)	–0.529(88)	0.5355(86)
Central naphthalene ring torsion angles							
C(6)–C(5)–C(10)–C(1)	–179.2(5) (179.2(5))	–177.0(5)	176.9(10)	175.8(3)	174.9(5)	174.8(6)	–174.5(6)
C(4)–C(5)–C(10)–C(9)	–178.4(6) (179.1(5))	–177.9(5)	–178.3(9)	173.8(3)	174.6(5)	173.4(6)	–175.1(6)

[a] Values in parentheses are for independent molecules. [b] vdW radii used for calculations: $r_{\text{vdW}}(\text{S}) = 1.80$ Å, $r_{\text{vdW}}(\text{Se}) = 1.90$ Å, $r_{\text{vdW}}(\text{Te}) = 2.06$ Å, $r_{\text{vdW}}(\text{Br}) = 1.85$ Å, $r_{\text{vdW}}(\text{I}) = 1.98$ Å.^[21] [c] Splay angle: Σ of the three bay region angles–360.

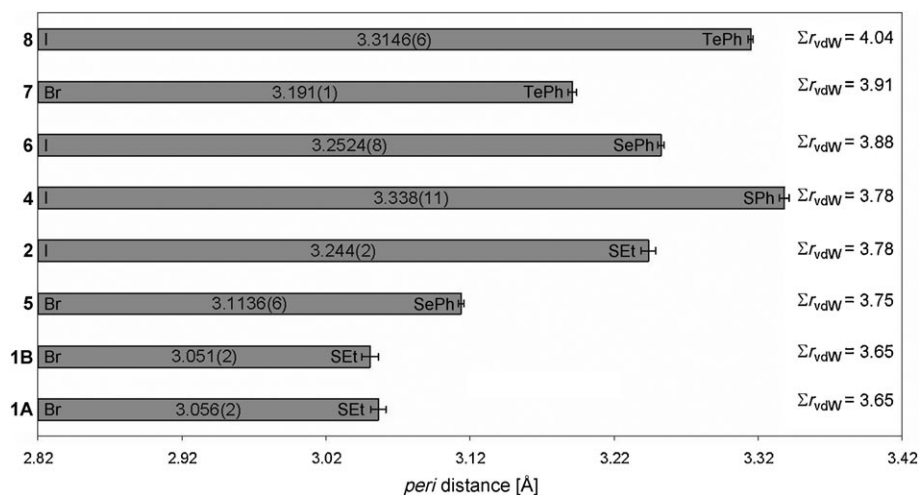


Figure 4. The *peri* distances for Nap[X][ER] derivatives **1–8**.

sides of the naphthalene least-squares plane in all seven derivatives. The distortion from this plane ranges from 0.01 to 0.54 Å. The least amount of steric strain is observed in **1**, as indicated by the relatively small displacement of the bromine and sulfur atoms ($\Sigma r_{vdW} = 3.65$ Å)^[24] from the naphthyl plane by -0.14 (0.01) and 0.04 Å (-0.04 Å; Figure 5). Out-of-plane distortion is observed to the greatest extent in **8** where the displacement of the large iodine and tellurium atoms ($\Sigma r_{vdW} = 4.04$ Å)^[24] is -0.42 and 0.54 Å, respectively (Figure 5). The positive splay angles of the seven derivatives (13.0–20.8°) indicate that considerable distortion has taken place in the bay area within the naphthyl plane. The X–C

formation of the naphthyl ring and ethyl group around the sulfur atom with respect to the C(Nap)–E–C(Et) plane. The increased congestion in the *peri* region of **2** results in a larger displacement of the *peri* atoms to opposite sides of the naphthalene least-squares plane compared with **1** (**1**: -0.14 (0.01) and 0.04 Å (-0.04 Å);^[18] **2**: 0.36 and -0.17 Å). Considerable distortion of the bay-region geometry within the naphthyl plane is observed in both compounds, but there is little difference between the splay angles (**1**: 14.5° (15.1°);^[18] **2**: 16.9°). The X–C and S–C bonds are tilted in opposite directions to minimise steric repulsion between the heavy atoms and alleviating *peri*-space crowding.^[26] The deviation of the central naphthalene ring torsion angles from planarity is more pronounced in **2** (≈ 2 –3°) than in **1**.

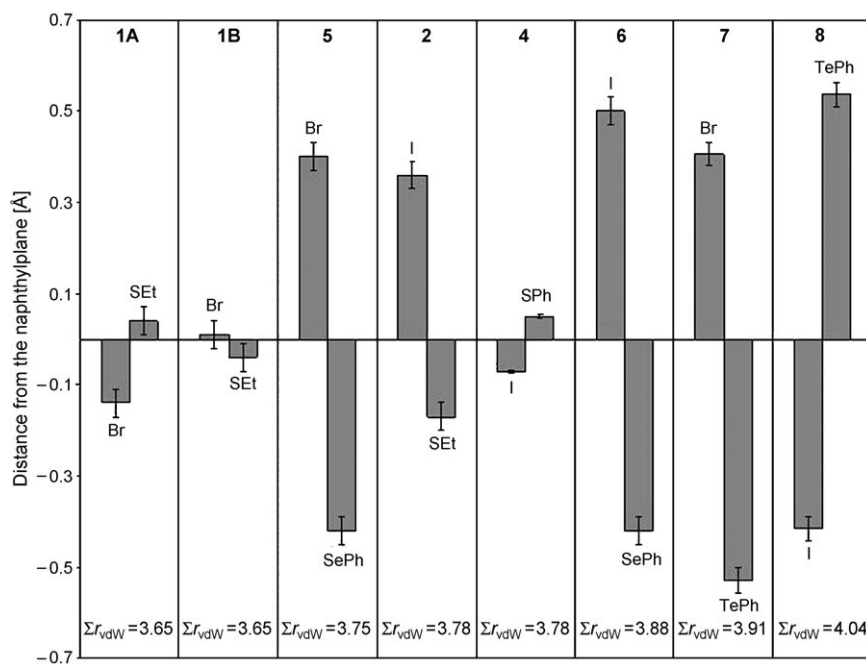


Figure 5. Out-of-plane displacement of the *peri* atoms to opposite sides of the naphthalene mean plane in Nap[X][ER] derivatives **1–8**.

and E–C bonds are forced apart to minimise the steric repulsion between the two bulky atoms and alleviate “*peri*-space crowding”.^[26]

The conformation and arrangement of the E(naphthyl) and E(phenyl) rings relative to the C(ar)–E(1)–C(ar) plane can be categorised from torsion angles θ and γ , respectively (see Table 2). When θ and γ approach 90°, the orientation is denoted axial and when the angles indicate a quasi-planar arrangement (close to 180°), they are termed equatorial.^[27]

Derivatives **1** and **2** display an equatorial–equatorial conformation of the naphthyl ring and ethyl group around the sulfur atom with respect to the C(Nap)–E–C(Et) plane. The increased congestion in the *peri* region of **2** results in a larger displacement of the *peri* atoms to opposite sides of the naphthalene least-squares plane compared with **1** (**1**: -0.14 (0.01) and 0.04 Å (-0.04 Å);^[18] **2**: 0.36 and -0.17 Å). Considerable distortion of the bay-region geometry within the naphthyl plane is observed in both compounds, but there is little difference between the splay angles (**1**: 14.5° (15.1°);^[18] **2**: 16.9°). The X–C and S–C bonds are tilted in opposite directions to minimise steric repulsion between the heavy atoms and alleviating *peri*-space crowding.^[26] The deviation of the central naphthalene ring torsion angles from planarity is more pronounced in **2** (≈ 2 –3°) than in **1**.

No major distortion of the naphthalene scaffold is observed in **1** with the maximum C–C–C–C torsion angle 1.6° for C(4)–C(5)–C(10)–C(9).^[18] As expected, the non-covalent I...S *peri* distance in **2** (3.2436(17) Å) is longer than the Br...S distance in **1** (3.0561(18) Å (3.050(2) Å)).^[18] These distances are shorter than the sum of the vdW radii for the interacting atoms by 0.59 Å (0.60 Å) and 0.54 Å for **1** and **2**, respectively.^[24] Br–C (1.90 Å), I–C (2.13 Å) and S–C (1.77–1.78 Å) bond lengths are within the usual ranges ((1.90 ± 0.05), (2.10 ± 0.05), (1.77 ± 0.05) Å)^[28] in both derivatives. The molecules of **1** pack in a herringbone array with no sig-

Table 2. Torsion angles [°] categorising the naphthalene and phenyl ring conformations in **1**, **2**, **4–8**.^[a]

	Naphthalene ring conformations		Phenyl ring conformations	
	C(10)–C(9)–E(1)–C(11)	Conformation	C(9)–E(1)–C(11)–C(12)	Conformation
1	$\theta = -177.2(5)$ (177.4(5))	Nap: equatorial	$(\gamma = 175.2(4) (-179.9(4)))$	(Et: equatorial)
2	$\theta = -174.3(5)$	Nap: equatorial	$(\gamma = 176.4(5))$	(Et: equatorial)
4	$\theta = 83.6(10)$	Nap: axial	$\gamma = 1.4(10)$	Ph: equatorial
5	$\theta = -159.2(3)$	Nap: equatorial	$\gamma = -96.0(3)$	Ph: axial
6	$\theta = -157.0(4)$	Nap: equatorial	$\gamma = -89.4(4)$	Ph: axial
7	$\theta = -160.0(6)$	Nap: equatorial	$\gamma = -99.4(5)$	Ph: axial
8	$\theta = -158.1(6)$	Nap: equatorial	$\gamma = -86.5(5)$	Ph: axial

[a] Values in parentheses are for independent molecules. Definitions: Nap: naphthalene ring E(1); Ph: E(1) phenyl ring; axial: perpendicular to C(ar)–E–C(ar) plane; equatorial: coplanar with C(ar)–E–C(ar) plane.

nificant π – π interactions. The shortest intermolecular S...S distance is 4.199(2) Å and there is a weak intermolecular C–H...Br interaction (C(22)–H(22a)···Br(1): H...Br = 3.025 Å, C–H...Br = 167°).^[18] No significant π – π interactions are observed in the packing structure of **2** but a short intermolecular I(1)···S(1A) interaction exists (3.504(1) Å).

The number, size and nature of atoms or groups attached to the *peri* atoms of 1,8-disubstituted naphthalenes has an important influence on the extent of steric strain that ultimately dictates the molecular geometry. The disparity between the electronic and steric affects of S(ethyl) and S(phenyl) moieties in derivatives **2** and **4** results in dissimilar intramolecular interactions, naphthalene distortion and structural arrangements. S(phenyl) derivative **4** arranges with a mixed axial–equatorial conformation of naphthyl and phenyl rings, respectively.

Although considerable distortion within the naphthyl plane occurs in both compounds, the splay of the X–C and E–C bonds is more pronounced in **4** to accommodate the larger substituent (**2**: 16.9°, **4**: 20.8°). Subsequently, the non-bonded intramolecular I...S(phenyl) *peri* distance (**4**: 3.338(11) Å) is noticeably longer than for the S(ethyl) derivative (**2**: 3.2436(17) Å), but still shorter than the sum of the vdW radii by 0.44 Å.^[24] The *peri* atoms essentially lie on the naphthyl plane in **4**, with only a minor displacement observed (–0.07 and 0.05 Å). Naphthalene skeletons for the two derivatives show similar deviations from planarity with central naphthalene ring torsion angles of around 2–3°. I–C (2.12 Å) and S–C (1.77 Å) bond lengths in **4** are within the usual ranges ((2.10 ± 0.05), (1.77 ± 0.05) Å).^[28] Although intermolecular short contacts exist, there is no significant overlap of phenyl or naphthalene rings and no π stacking in the molecular structure of **4**.

The increasing magnitude of the *peri* atoms (BrSe 3.75 Å, ISe 3.88 Å, BrTe 3.91 Å, ITe 4.04 Å)^[24] in derivatives **5–8** causes an escalating degree of steric congestion in the bay region. Steric strain resulting from repulsive X...E interac-

tions transpires, forcing the naphthalene geometry to distort further from ideal.^[3] Non-bonded interatomic *peri* distances (X...E) display a general increase when larger atoms occupy the close-contact 1,8-positions. X...E separations for **5** (3.1136(6) Å), **6** (3.2524(8) Å), **7** (3.1909(10) Å) and **8** (3.3146(6) Å) are in all cases less than the respective sum of the vdW radii for the two interacting atoms; for each distance this is between 82 and 84 % of the vdW sum (Table 1). The increase in steric congestion is accompanied by a larger positive splay of the X–C and E–C bonds within the naphthyl plane with angles increasing from 13.0° in **5** to 16.2° in **8**.

Displacement of the halogen and chalcogen atoms from the naphthalene best plane is, however, comparable for all four derivatives with distances of between 0.40 and 0.54 Å from the plane. The naphthalene unit in each derivative displays considerable buckling, with a similar deviation from planarity observed throughout the series; central naphthalene ring C–C–C–C torsion angles lie in the range of 4.2 to 6.6°. Br–C (1.919(3), 1.917(6) Å), I–C (2.122(4), 2.108(6) Å), Se–C (1.948(3), 1.958(4) Å) and Te–C (2.153(6), 2.151(6) Å) bond lengths are within the usual ranges ((1.90 ± 0.05), (2.10 ± 0.05), (1.93 ± 0.05) and (2.12 ± 0.05) Å, respectively)^[28] in all four compounds. Similar packing with expected intermolecular short contacts is observed throughout the series. There is no significant overlap of phenyl or naphthyl rings and no π – π stacking.

Analogues **5–8** display a different geometry compared with **4**, adopting a mixed equatorial–axial conformation of naphthyl and phenyl rings respectively in each case (Table 2). The difference between the two conformations is illustrated by Figure 6, which shows a view of the geometrical arrangements along the E(1)–C(9) bond; axial naphthalene conformation in **4** and equatorial naphthalene conformation in **5–8**.

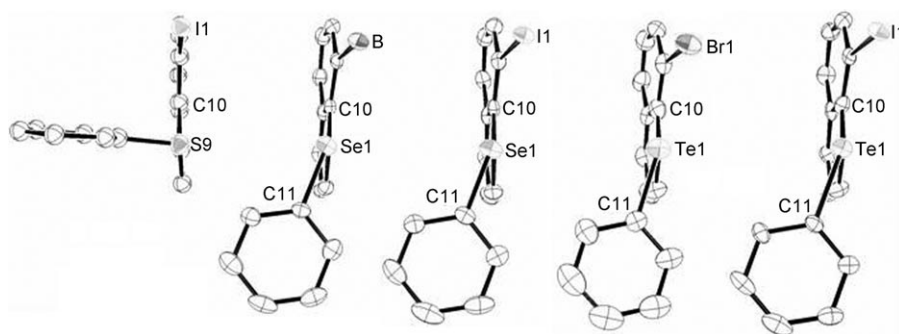


Figure 6. The crystal structures of **4** and **5–8** viewed along the E(1)–C(9) bond, showing the difference in naphthyl and phenyl ring conformations.

Steric strain operating between the *peri* atoms in **4** and **5–8** is dominated by the repulsion of p-type lone pairs, which thus have a big influence on non-bonded X...E distances. Compared with derivatives **5–8**, compound **4** experiences a larger than expected amount of steric strain as illustrated by a *peri* distance (3.338(11) Å) significantly larger than S(ethyl) analogue **2** (3.0561(18) Å) and comparable to **8** (3.3146(6) Å) containing much larger iodine and tellurium atoms. The extent of steric strain occurring in **4** can be explained by the axial conformation of the E(naphthyl) ring. When torsion angles θ (see Table 2) approach 90°, the axis of the p orbitals of the chalcogen atom lie in the plane of the aromatic system and repulsion is relatively high.^[27] Conversely, the torsion angles θ for **5–8** approach 180° (E(naphthyl) conformation being equatorial), the p orbitals are arranged parallel and vertical to the aromatic plane and less lone pair–lone pair repulsion is observed.^[27]

The possibility of attractive non-covalent X...E interactions occurring in **5–8** is heightened by the presence of a quasi-linear X...E–C alignment of atoms. When the heteroatom orbitals are closely located and align linearly, it is possible for promotion of a halogen lone pair into the antibonding $\sigma^*(\text{E}–\text{C})$ orbital^[29] to form a weak unsymmetrical hypervalent interaction. This attractive σ -type (X)... $\sigma^*(\text{E}–\text{C})$ alignment is known as a three-centre–four-electron (3c–4e) interaction and can influence the conformation of the molecule.^[2,8–12,30,31]

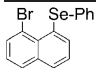
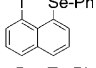
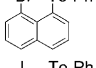
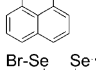
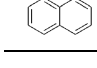
Nakanishi et al. have investigated non-bonded intramolecular interactions in a series of sterically crowded naphthalenes that contain the 8-G-1-(*p*-YC₆H₄Se)C₁₀H₆ structural motif.^[2,8–12] Compounds in which G = Cl or Br (such as **5**) were found to adopt type B structures (Se–C bond located on the naphthyl plane) irrespective of what occupies the Y position, and the linear non-bonded G...Se–C arrangement was concluded to result from the occurrence of a 3c–4e bond.^[2,8–12,30,31]

Derivatives **6–8** also adopt the type B structure with E–C bonds lying close to the naphthalene plane (Figure 7). The E(phenyl) moieties sit in similar locations in all four derivatives and produce a quasi-linear arrangement of the type X...EC with angles approaching 180° (**5**: Br...Se–C 175.7°, **6**: I...Se–C 174.3°, **7**: Br...Te–C 173.1°, **8**: I...Te–C 175.1°; Figure 7).

To try and assess the possibility of direct X...E bonding interactions that would indicate an onset of 3c–4e bonding, density functional theory computations were performed for derivatives **5–8** at the B3LYP/6-31+G* level. The Wiberg bond index (WBI),^[32] which measures the covalent bond

order, was calculated and found to increase from 0.05 for **5** to 0.08 for **8**, but indicates a very minor interaction taking place between the non-bonded atoms in these compounds (Table 3). For comparison, the fully covalent S–S single bond in naphtho[1,8-*cd*][1,2]dithiole has a WBI of 0.99 at the same level.

Table 3. Results of ab initio MO calculations performed on **5–8** evaluated at the B3LYP/6-31+G* level by using X-ray and fully optimised geometries.

	X...Y (exptl)	WBI	X...Y (calcd)	WBI
	3.114	0.05	3.172	0.05
	3.252	0.06	3.336	0.05
	3.191	0.07	3.266	0.07
	3.426	0.08	3.427	0.08
	2.542 (2.516) ^[33]	0.52 (0.55)	2.775	0.37

These results illustrate that more pronounced interactions could be expected as the neighbouring atoms become larger. Even stronger interactions can occur when one of the Se atoms carries an acceptor and indeed, if the equatorial Ph group on Se1 in 1,8-bis(phenylselanyl)naphthalene is replaced with Br, Se–Se distances as short as 2.516 Å have been observed.^[33] A B3LYP computation for the latter molecule from the X-ray structure gives a WBI of 0.55, suggesting a large extent of 3c–4e bonding in this case. Judging from the refined halogen–chalcogen distances, none of the species in the present study comes close to such a bonding situation.

Conclusion

The work presented herein complements our previous work on 1,8-chalcogen naphthalene derivatives,^[16] builds on the knowledge of molecular naphthalene distortion and contributes to the understanding of weak intramolecular interactions acting between heavy atoms when constrained at the close 1,8-positions.^[1] The insertion of increasingly large atoms at the *peri* positions of compounds **1–8** enhances the repulsive steric strain operating in the naphthalene skeleton. Relief through molecular distortion transpires and is generally observed to a greater extent as the overall combined *peri*-atom size increases (Figures 3 and 5); however, the number, size and nature of substituents bound to the *peri* atoms can also affect the conformation of the molecule. The degree of deviation from an ideal geometry^[3] can be quantified by the *peri* distance, which encapsulates all molecular distortions in one entity.

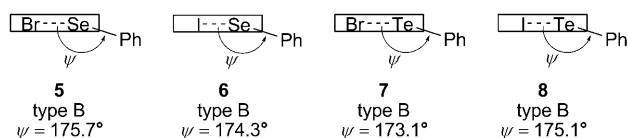


Figure 7. The orientation of the E(phenyl) groups and type of structure of **5–8** and the quasi-linear arrangements.^[1h,2,8,9,11]

The largest *peri* distances were found in **4** and **8**; the large tellurium and iodine atoms in **8** ($\Sigma r_{\text{vdW}} = 4.04 \text{ \AA}$)^[24] experience a greater degree of steric congestion, whereas the axial conformation of the naphthyl ring relative to the C(ar)-E-C(ar) plane in **4** results in greater repulsion between lone pairs.^[27] The shortest *peri* gap is observed in **1**, which contains the two smallest (sulfur and bromine) substituents ($\Sigma r_{\text{vdW}} = 3.65 \text{ \AA}$).^[24] In all derivatives the non-bonded distance was shorter than the sum of the vdW radii for the two *peri* atoms by 12–18%.

The contrasting conformation of **4** is the most notable difference observed in the series of compounds. Compounds **5**–**8** all adopt the type B structure with E–C_{ph} bonds aligning close to the naphthyl plane^[1h,2,8,9,11] and a mixed equatorial–axial arrangement of naphthyl and phenyl rings around the chalcogen atom,^[27] whereas **4** is arranged with the S–C_{ph} bond perpendicular to the plane and adopts an axial–equatorial conformation for the naphthyl and phenyl rings.^[1h,2,8,9,11,27] This indicates that chalcogen p-type lone pair repulsion is more dominant in **4** compared with **5**–**8**.^[27]

The orientation of the E(phenyl) moiety in **5**–**8** allows for a possible attractive 3c–4e interaction due to a quasi-linear arrangement of the type X···E–C_{ph}. In each of the four derivatives angles approach 180° (173.1–175.7°) and non-bonded X···E distances are all shorter than the sum of the respective vdW radii. Ab initio MO calculations performed at the B3LYP/6-31+G* level on all four derivatives revealed Wiberg bond index (WBI)^[32] values of 0.05 to 0.08, which indicate that only a very minor interaction exists between the non-bonded atoms and the refined halogen–chalcogen distances don't come close to those of a 3c–4e interaction.

Experimental Section

All experiments were carried out under an oxygen- and moisture-free nitrogen atmosphere by using standard Schlenk techniques and glassware. Reagents were obtained from commercial sources and used as received. Dry solvents were collected from an MBraun solvent system. 1,8-Dibromonaphthalene **11**^[22] and 1,8-diiodonaphthalene **12**^[23] were prepared by standard diazotisation reactions of 1,8-diaminonaphthalene. Elemental analyses were performed by the University of St Andrews School of Chemistry Microanalysis Service. IR spectra were recorded as KBr discs in the range of 4000–300 cm^{−1} by using a Perkin–Elmer System 2000 Fourier transform spectrometer. ¹H and ¹³C NMR spectra were recorded by using a Jeol GSX 270 MHz spectrometer with $\delta(\text{H})$ and $\delta(\text{C})$ referenced to external tetramethylsilane. ⁷⁷Se and ¹²⁵Te NMR spectra were recorded by using a Jeol GSX 270 MHz spectrometer with $\delta(\text{Se})$ and $\delta(\text{Te})$ referenced to external dimethylselenide and diphenyl ditelluride, respectively. Assignments of ¹³C and ¹H NMR spectra were made with the help of H–H COSY and HSQC experiments. All measurements were performed at 25°C. All values reported for NMR spectroscopy are in parts per million (ppm). Coupling constants (*J*) are given in Hertz (Hz). Mass spectrometry was performed by the University of St Andrews Mass Spectrometry Service. Electron impact mass spectrometry (EIMS) and chemical ionisation mass spectrometry (CIMS) was carried out by using a Micromass GCT orthogonal acceleration time-of-flight mass spectrometer. Electrospray mass spectrometry (ESMS) was carried out on a Micromass LCT orthogonal accelerator time-of-flight mass spectrometer.

Synthesis of 1-bromo-8-(ethylsulfanyl)naphthalene (Nap[Br][SEt]; 1) from 9: A solution of *n*-butyllithium (2.5 M) in hexane (0.9 mL, 2.2 mmol) was added dropwise to a solution of 1,8-dibromonaphthalene (0.6 g, 2.2 mmol) in diethyl ether (10 mL) at −78°C. The mixture was stirred at this temperature for 1 h, after which a solution of diethyl disulfide (0.3 g, 0.3 mL, 2.2 mmol) was added dropwise. The resulting mixture was stirred at −78°C for a further 1 h, then washed with 0.1 M sodium hydroxide (2 × 20 mL). The organic layer was dried with magnesium sulfate, concentrated under reduced pressure, and the residual yellow oil was purified by column chromatography on silica gel (hexane) to give a brown solid. Recrystallisation from dichloromethane/pentane gave the product as colourless crystals (0.3 g, 43%). M.p./b.p. 47–49°C (lit.: 47–48°C^[7]); ¹H NMR (270 MHz, CDCl₃, 25°C, TMS): $\delta = 7.75$ (dd, ³*J*(H,H) = 7.4 Hz, ⁴*J*(H,H) = 1.2 Hz, 1H; nap 4-H), 7.68 (dd, ³*J*(H,H) = 8.1 Hz, ⁴*J*(H,H) = 1.1 Hz, 1H; nap 2-H), 7.55 (dd, ³*J*(H,H) = 8.0 Hz, ⁴*J*(H,H) = 1.1 Hz, 1H; nap 5-H), 7.42 (dd, ³*J*(H,H) = 7.5 Hz, ⁴*J*(H,H) = 1.0 Hz, 1H; nap 7-H), 7.28 (t, ³*J*(H,H) = 7.8 Hz, 1H; nap 6-H), 7.14 (t, ³*J*(H,H) = 7.8 Hz, 1H; nap 3-H), 2.92 (q, ³*J*(H,H) = 7.3 Hz, 2H; CH₂), 1.28 ppm (t, ³*J*(H,H) = 7.4 Hz, 3H; CH₃); ¹³C NMR (67.9 MHz, CDCl₃, 25°C, TMS): $\delta = 136.9$ (q), 136.1 (q), 134.2 (s), 130.8 (q), 129.5 (s), 127.8 (s), 127.1 (s), 126.2 (s), 125.9 (s), 119.4 (q), 30.0 (s; CH₂), 13.4 ppm (s; CH₃); IR (KBr disk): $\tilde{\nu}_{\text{max}} = 3056$ w, 2971 w, 2925 w, 2851 w, 1923 w, 1544 vs, 1511 w, 1493 w, 1461 w, 1434 w, 1416 w, 1356 s, 1308 s, 1256 w, 1191 vs, 1148 s, 1057 w, 967 s, 857 s, 801 vs, 702 s, 545 w, 439 cm^{−1} w; MS (CI⁺): *m/z* (%): 266.0 (100) [M+H⁺]; elemental analysis calcd (%) for C₁₂H₁₁BrS: C 54.0, H 4.2; found: C 54.1, H 4.3.

Synthesis of 1-iodo-8-(ethylsulfanyl)naphthalene (Nap[I][SEt]; 2) from 10: A solution of *n*-butyllithium (2.5 M) in hexane (0.9 mL, 2.3 mmol) was added dropwise to a solution of 1,8-diiodonaphthalene (0.88 g, 2.3 mmol) in diethyl ether (10 mL) at −78°C. The mixture was stirred at this temperature for 1 h, after which a solution of diethyl disulfide (0.28 g, 0.3 mL, 2.3 mmol) was added dropwise. The resulting solution was stirred at −78°C for a further 1 h and then washed with 0.1 M sodium hydroxide (2 × 20 mL). The organic layer was dried with magnesium sulfate, concentrated under reduced pressure, and the residual brown oil was purified by column chromatography on silica gel (hexane) to give a yellow solid. Recrystallisation from dichloromethane/pentane gave the product as colourless crystals (0.3 g, 42%). M.p./b.p. 53–55°C; ¹H NMR (270 MHz, CDCl₃, 25°C, TMS): $\delta = 8.26$ (dd, ³*J*(H,H) = 7.4 Hz, ⁴*J*(H,H) = 1.3 Hz, 1H; nap 4-H), 7.74 (dd, ³*J*(H,H) = 8.1 Hz, ⁴*J*(H,H) = 1.2 Hz, 1H; nap 2-H), 7.67–7.58 (m, 2H; nap 5,7-H), 7.31 (t, ³*J*(H,H) = 7.7 Hz, 1H; nap 6-H), 7.02–6.95 (m, 1H; nap 3-H), 2.89 (q, ³*J*(H,H) = 7.4 Hz, 2H; SCH₂), 1.22 ppm (t, ³*J*(H,H) = 7.4 Hz, 3H; SCH₂CH₃); ¹³C NMR (67.9 MHz, CDCl₃, 25°C, TMS): $\delta = 143.3$ (s), 131.3 (s), 130.4 (s), 128.7 (s), 126.8 (s), 125.6 (s) 31.9 (s; CH₂), 13.6 ppm (s; CH₃); IR (KBr disk): $\tilde{\nu}_{\text{max}} = 3412$ br, 3051 w, 2965 w, 2924 s, 1539 s, 1500 w, 1440 w, 1372 w, 1354 w, 1308 w, 1259 s, 1190 s, 1142 w, 1096 w, 1049 w, 1020 w, 963 w, 942 w, 898 w, 849 w, 790 vs, 762 vs, 689 w, 642 w, 561 w, 538 w, 401 cm^{−1} w; MS (EI⁺): *m/z* (%): 314.0 (22) [M]⁺, 254.0 (72) [M–SEt]⁺; elemental analysis calcd (%) for C₁₀H₆I₂: C 45.9, H 3.5; found: C 46.7, H 3.1.

Synthesis of 1-bromo-8-(phenylsulfanyl)naphthalene (Nap[Br][SPh]; 3) from 9: A solution of *n*-butyllithium (2.5 M) in hexane (0.9 mL, 2.3 mmol) was added dropwise to a solution of 1,8-dibromonaphthalene (0.67 g, 2.3 mmol) in diethyl ether (15 mL) at −78°C. The mixture was stirred at this temperature for 1 h, after which a solution of diphenyl disulfide (0.51 g, 2.3 mmol) in diethyl ether (15 mL) was added dropwise. The resulting mixture was stirred at −78°C for a further 1 h, then washed with 0.1 M sodium hydroxide (2 × 45 mL). The organic layer was dried with magnesium sulfate, concentrated under reduced pressure, and the residual brown oil was purified by column chromatography on silica gel (hexane/ethyl acetate 20:1) to give the product as a brown oil (0.7 g, 51%). ¹H NMR (270 MHz, CDCl₃, 25°C, TMS): $\delta = 7.80$ (dd, ³*J*(H,H) = 7.4 Hz, ⁴*J*(H,H) = 1.3 Hz, 1H; nap 4-H), 7.73 (dd, ³*J*(H,H) = 8.2 Hz, ⁴*J*(H,H) = 1.1 Hz, 1H; nap 2-H), 7.65 (dd, ³*J*(H,H) = 8.1 Hz, ⁴*J*(H,H) = 1.2 Hz, 1H; nap 5-H), 7.55 (dd, ³*J*(H,H) = 7.5 Hz, ⁴*J*(H,H) = 1.3 Hz, 1H; nap 7-H), 7.28–7.14 ppm (m, 7H; nap 3,6-H, SPh 2–6-H); ¹³C NMR (67.9 MHz, CDCl₃, 25°C, TMS): $\delta = 137.6$ (s), 133.2 (s), 131.9 (s), 129.53 (s), 129.49 (s), 128.9 (s), 127.4 (s), 126.4 (s), 126.1 ppm (s).

Synthesis of 1-iodo-8-(phenylsulfanyl)naphthalene (Nap[I][SPh]; 4) from 10: A solution of *n*-butyllithium (2.5 M) in hexane (0.5 mL, 1.2 mmol) was added dropwise to a solution of 1,8-diiodonaphthalene (0.47 g, 1.2 mmol) in diethyl ether (15 mL) at -78°C . The mixture was stirred at this temperature for 1 h, after which a solution of diphenyl disulfide (0.27 g, 1.2 mmol) in diethyl ether (15 mL) was added dropwise. The resulting mixture was stirred at -78°C for a further 1 h, then washed with 0.1 M sodium hydroxide (2×45 mL). The organic layer was dried with magnesium sulfate, concentrated under reduced pressure and the residual yellow oil was purified by column chromatography on silica gel (hexane); the resulting yellow solid was recrystallised from dichloromethane/pentane to give the product as colourless crystals (0.1 g, 26 %). M.p./b.p. $47\text{--}49^{\circ}\text{C}$; ^1H NMR (270 MHz, CDCl_3 , 25°C , TMS): $\delta = 8.27$ (dd, $^3J(\text{H,H}) = 7.4$ Hz, $^4J(\text{H,H}) = 1.3$ Hz, 1H; nap 4-H), 7.79 (dd, $^3J(\text{H,H}) = 8.1$ Hz, $^4J(\text{H,H}) = 1.2$ Hz, 1H; nap 2-H), 7.75 (dd, $^3J(\text{H,H}) = 8.2$ Hz, $^4J(\text{H,H}) = 1.3$ Hz, 1H; nap 5-H), 7.64 (dd, $^3J(\text{H,H}) = 7.3$ Hz, $^4J(\text{H,H}) = 1.4$ Hz, 1H; nap 7-H), 7.33–7.26 (m, 1H, nap 6-H), 7.21–6.97 ppm (m, 6H, nap 3-H, SPh 2–6-H); ^{13}C NMR (67.9 MHz, CDCl_3 , 25°C , TMS): $\delta = 143.9$ (s), 136.4 (s), 130.7 (s), 130.5 (s), 129.7 (s), 129.3 (s), 127.1 (s), 126.3 (s), 126.0 ppm (s); IR (KBr disk): $\tilde{\nu}_{\text{max}} = 3442$ br, 3056 w, 2955 s, 2924 s, 2848 w, 1937 w, 1790 w, 1719 w, 1654 w, 1578 s, 1535 s, 1474 s, 1432 s, 1346 w, 1314 w, 1261 s, 1187 s, 1080 vs, 1022 vs, 959 w, 891 w, 850 w, 815 vs, 755 vs, 733 vs, 688 s, 613 w, 566 w, 516 w, 462 w, 400 cm^{-1} w; MS (ES^+): m/z (%): 384.80 (100) [$\text{M} + \text{Na}$] $^+$; elemental analysis calcd (%) for $\text{C}_{16}\text{H}_{11}\text{IS}$: C 53.0, H 3.1; found: C 53.0, H 3.4.

Synthesis of 1-bromo-8-(phenylselenanyl)naphthalene (Nap[Br][SePh]; 5) from 9: A solution of *n*-butyllithium (2.5 M) in hexane (7 mL, 0.018 mol) was added dropwise to a solution of 1,8-dibromonaphthalene (5.0 g, 0.018 mol) in diethyl ether (35 mL) at -78°C . The mixture was stirred at this temperature for 1 h, after which a solution of diphenyl diselenide (5.45 g, 0.018 mol) in diethyl ether (10 mL) was added dropwise. The resulting mixture was stirred at -78°C for a further 1 h, then washed with 0.1 M sodium hydroxide (2×45 mL). The organic layer was dried with magnesium sulfate and concentrated under reduced pressure. The residual brown oil was purified by column chromatography on silica gel (hexane/dichloromethane 20:1) and the resulting green/brown solid was recrystallised from dichloromethane/pentane to give the product as colourless crystals (4.0 g, 63 %). M.p./b.p. $77\text{--}79^{\circ}\text{C}$ (lit.: 78°C); ^1H NMR (270 MHz, CDCl_3 , 25°C , TMS): $\delta = 7.88$ (dd, $^3J(\text{H,H}) = 7.4$ Hz, $^4J(\text{H,H}) = 1.2$ Hz, 1H; nap 4-H), 7.81 (d, $^3J(\text{H,H}) = 8.1$ Hz, 1H; nap 2-H), 7.74–7.59 (m, 3H; nap 5-H, SPh 2,6-H), 7.49–7.36 (m, 3H; SPh 3–5-H), 7.34–7.22 (m, 2H; nap 3,7-H), 7.19–7.09 ppm (m, 1H; nap 6-H); ^{13}C NMR (67.9 MHz, CDCl_3 , 25°C , TMS): $\delta = 137.1$ (q), 136.8 (s), 133.5 (q), 133.4 (s), 132.1 (q), 131.7 (q), 130.9 (s), 130.0 (s), 129.4 (s), 128.9 (s), 127.6 (s), 126.4 (s), 126.2 (s), 120.6 ppm (q); ^{77}Se NMR (51.5 MHz, CDCl_3 , 25°C , PhSeSePh): $\delta = 447.8$ ppm; IR (KBr disk): $\tilde{\nu}_{\text{max}} = 3058$ w, 2955 w, 2925 w, 1787 w, 1573 w, 1541 s, 1473 w, 1462 w, 1434 s, 1353 w, 1299 w, 1269 w, 1187 s, 1139 s, 1089 w, 1061 w, 1020 w, 997 w, 953 w, 903 w, 841 w, 806 vs, 746 vs, 691 vs, 557 w, 533 w, 476 w, 436 w, 315 cm^{-1} w; MS (EI^+): m/z (%): 361.9 (100) [M] $^+$; elemental analysis calcd (%) for $\text{C}_{16}\text{H}_{11}\text{BrSe}$: C 53.0, H 3.1; found: C 52.6, H 3.6.

Synthesis of 1-iodo-8-(phenylselenanyl)naphthalene (Nap[I][SePh]; 6) from 10: A solution of *n*-butyllithium (2.5 M) in hexane (0.5 mL, 1.3 mmol) was added dropwise to a solution of 1,8-diiodonaphthalene (0.49 g, 1.3 mmol) in diethyl ether (15 mL) at -78°C . The mixture was stirred at this temperature for 1 h, after which a solution of diphenyl diselenide (0.40 g, 1.3 mmol) in diethyl ether (15 mL) was added dropwise. The resulting mixture was stirred at -78°C for a further 1 h, then washed with 0.1 M sodium hydroxide (2×45 mL). The organic layer was dried with magnesium sulfate and concentrated under reduced pressure. The crude brown solid was purified by column chromatography on silica gel (hexane) and recrystallised from dichloromethane/pentane to give the product as colourless crystals (0.3 g, 60 %). M.p./b.p. $56\text{--}58^{\circ}\text{C}$; ^1H NMR (270 MHz, CDCl_3 , 25°C , TMS): $\delta = 8.22$ (dd, $^3J(\text{H,H}) = 7.4$ Hz, $^4J(\text{H,H}) = 1.3$ Hz, 1H; nap 4-H), 7.74 (dd, $^3J(\text{H,H}) = 8.1$ Hz, $^4J(\text{H,H}) = 1.0$ Hz, 1H; nap 2-H), 7.57 (dd, $^3J(\text{H,H}) = 8.0$ Hz, $^4J(\text{H,H}) = 1.1$ Hz, 1H; nap 5-H), 7.49–7.43 (m, 2H; SPh 2,6-H), 7.35 (dd, $^3J(\text{H,H}) = 7.5$ Hz, $^4J(\text{H,H}) = 1.2$ Hz, 1H; nap 7-H), 7.32–7.24 (m, 3H; SPh 3–5-H), 7.12–6.99 ppm (m, 2H; nap 3,6-H); ^{13}C NMR (67.9 MHz, CDCl_3 , 25°C , TMS): $\delta = 142.2$ (s), 135.6 (s),

133.1 (s), 130.2 (s), 129.8 (s), 128.6 (s), 128.4 (s), 126.8 (s), 126.3 ppm (s); ^{77}Se NMR (51.5 MHz, CDCl_3 , 25°C , PhSeSePh): $\delta = 430.8$ ppm; IR (KBr disk): $\tilde{\nu}_{\text{max}} = 3442$ br, 3051 s, 1961 w, 1911 w, 1887 w, 1778 w, 1633 w, 1571 s, 1537 vs, 1488 w, 1473 s, 1434 s, 1349 s, 1311 s, 1299 s, 1272 w, 1185 s, 1133 s, 1089 w, 1062 s, 1018 s, 997 w, 947 w, 897 w, 829 w, 804 vs, 742 vs, 691 vs, 607 w, 551 w, 524 w, 474 s, 427 w, 306 cm^{-1} w; MS (EI^+): m/z (%): 409.9 (51) [M] $^+$; elemental analysis calcd (%) for $\text{C}_{16}\text{H}_{11}\text{ISe}$: C 47.0, H 2.7; found: C 47.0, H 2.5.

Synthesis of 1-bromo-8-(phenyltelluro)naphthalene (Nap[Br][TePh]; 7) from 9: A solution of *n*-butyllithium (2.5 M) in hexane (0.5 mL, 1.9 mol) was added dropwise to a solution of 1,8-dibromonaphthalene (0.55 g, 1.9 mol) in diethyl ether (35 mL) at -78°C . The mixture was stirred at this temperature for 1 h after which a solution of diphenyl ditelluride (0.79 g, 1.9 mol) in diethyl ether (20 mL) was added dropwise to the mixture. The resulting mixture was stirred at -78°C for a further 1 h. The reaction mixture was washed with 0.1 M sodium hydroxide (2×45 mL). The organic layer was dried with magnesium sulfate, concentrated under reduced pressure and the resulting golden solid was purified by column chromatography on silica gel (ethyl acetate/hexane 1:20). Recrystallisation from dichloromethane/pentane afforded the product as colourless crystals (0.3 g, 32 %). M.p./b.p. $105\text{--}107^{\circ}\text{C}$; ^1H NMR (270 MHz, CDCl_3 , 25°C , TMS): $\delta = 8.02\text{--}7.92$ (m, 2H; TePh 2,6-H), 7.80 (dd, $^3J(\text{H,H}) = 7.5$ Hz, $^4J(\text{H,H}) = 1.3$ Hz, 1H; nap 5-H), 7.76 (dd, $^3J(\text{H,H}) = 8.3$ Hz, $^4J(\text{H,H}) = 1.1$ Hz, 1H; nap 7-H), 7.63–7.55 (m, 1H; nap 4-H), 7.52–7.41 (m, 2H; nap 2-H, TePh 4-H), 7.41–7.31 (m, 2H; TePh 3,5-H), 7.28–7.20 (m, 1H; nap 6-H), 7.02 ppm (t, $^3J(\text{H,H}) = 7.7$ Hz, 1H; nap 3-H); ^{13}C NMR (67.9 MHz, CDCl_3 , 25°C , TMS): $\delta = 141.3$ (s), 137.3 (q), 135.4 (s), 134.0 (q), 132.5 (s), 130.2 (s), 129.8 (s), 129.2 (s), 128.2 (s), 126.9 (s), 126.1 (s), 122.5 (q), 121.2 (q), 117.6 ppm (q); ^{125}Te NMR (81.2 MHz, CDCl_3 , 25°C , PhTeTePh): $\delta = 731.2$ ppm; IR (KBr disk): $\tilde{\nu}_{\text{max}} = 3409$ w, 3056 w, 2921 w, 2584 w, 2365 w, 2343 w, 1723 w, 1659 w, 1640 w, 1568 w, 1535 s, 1469 s, 1431 s, 1385 w, 1350 s, 1329 w, 1299 w, 1262 w, 1185 s, 1133 s, 1059 s, 1015 s, 996 s, 946 w, 908 w, 834 s, 804 vs, 739 vs, 692 s, 602 w, 553 w, 527 w, 459 cm^{-1} s; MS (CI^+): m/z (%): 411.9 (85) [M] $^+$, 334.9 (45) [$\text{M} - \text{Ph}$] $^+$; elemental analysis calcd (%) for $\text{C}_{16}\text{H}_{11}\text{BrTe}$: C 46.8, H 2.7; found: C 46.8, H 2.7.

Synthesis of 1-iodo-8-(phenyltelluro)naphthalene (Nap[I][TePh]; 8) from 10: A solution of *n*-butyllithium (2.5 M) in hexane (0.5 mL, 1.1 mol) was added dropwise to a solution of 1,8-diiodonaphthalene (0.43 g, 1.1 mol) in diethyl ether (35 mL) at -78°C . The mixture was stirred at this temperature for 1 h, after which a solution of diphenyl ditelluride (0.46 g, 1.1 mol) in diethyl ether (20 mL) was added dropwise. The resulting mixture was stirred at -78°C for a further 1 h, then washed with 0.1 M sodium hydroxide (2×45 mL). The organic layer was dried with magnesium sulfate, concentrated under reduced pressure and the resulting golden solid was purified by column chromatography on silica gel (ethyl acetate/hexane 1:20). Recrystallisation of the golden solid from dichloromethane/pentane gave the product as colourless crystals (0.09 g, 18 %). M.p./b.p. $109\text{--}111^{\circ}\text{C}$; ^1H NMR (270 MHz, CDCl_3 , 25°C , TMS): $\delta = 8.11$ (dd, $^3J(\text{H,H}) = 7.4$ Hz, $^4J(\text{H,H}) = 1.2$ Hz, 1H; nap 4-H), 7.79–7.73 (m, 2H; TePh 2,6-H), 7.68 (dd, $^3J(\text{H,H}) = 8.1$ Hz, $^4J(\text{H,H}) = 1.0$ Hz, 1H; nap 2-H), 7.53–7.46 (m, 2H; nap 5,7-H), 7.34–7.27 (m, 1H; TePh 4-H), 7.25–7.18 (m, 2H; TePh 3–5-H), 7.02–6.95 (m, 1H; nap 3-H), 6.93 ppm (m, 1H; nap 6-H); ^{13}C NMR (67.9 MHz, CDCl_3 , 25°C , TMS): $\delta = 141.0$ (s), 140.5 (s), 137.0 (s), 130.5 (s), 130.0 (s), 128.8 (s), 128.8 (s), 126.7 (s), 126.6 ppm (s); ^{125}Te NMR (81.2 MHz, CDCl_3 , 25°C , PhTeTePh): $\delta = 698.3$ ppm; IR (KBr disk): $\tilde{\nu}_{\text{max}} = 3422$ br, 3051 w, 2923 s, 2851 w, 1566 w, 1529 s, 1467 w, 1430 s, 1381 w, 1344 w, 1296 w, 1256 w, 1182 w, 1130 s, 1056 w, 1013 w, 996 w, 942 w, 905 w, 823 w, 802 vs, 739 vs, 691 s, 663 w, 546 w, 520 w, 457 cm^{-1} s; MS (ES^+): m/z (%): 490.78 (100) [$\text{M} + \text{OMe}$] $^+$; elemental analysis calcd (%) for $\text{C}_{16}\text{H}_{11}\text{ITe}$: C 42.0, H 2.4; found: C 42.6, H 2.6.

Crystal structure analyses: X-ray crystal structures for compounds **1**, **5** and **6** were determined at $-148(1)^{\circ}\text{C}$ by using a Rigaku SCXmini CCD area detector with graphite monochromated MoK_{α} radiation ($\lambda = 0.71073\text{ \AA}$). The data were corrected for Lorentz, polarisation and absorption. Data for compound **4** were collected at $-180(1)^{\circ}\text{C}$ by using a Rigaku MM007 High brilliance RA generator (MoK_{α} radiation, confocal optic) and Mercury CCD system. At least a full hemisphere of data was

Table 4. Crystallographic data for compounds **2**, **4** and **6–8**.

	2	4	6	7	8
empirical formula	C ₁₂ H ₁₁ IS	C ₁₆ H ₁₁ IS	C ₁₆ H ₁₁ ISe	C ₁₆ H ₁₁ BrTe	C ₁₆ H ₁₁ ITe
<i>M_r</i>	314.18	362.21	409.13	410.77	457.77
<i>T</i> [°C]	−148(1)	20(1)	−148(1)	−148(1)	−148(1)
colour, habit	colourless, prism	colourless, platelet	colourless, prism	colourless, prism	colourless, prism
crystal size [mm ³]	0.21 × 0.09 × 0.06	0.10 × 0.10 × 0.10	0.30 × 0.24 × 0.12	0.09 × 0.06 × 0.06	0.15 × 0.09 × 0.09
crystal system	orthorhombic	orthorhombic	triclinic	monoclinic	monoclinic
<i>a</i> [Å]	7.768(2)	10.204(4)	7.8388(7)	12.556(3)	12.437(8)
<i>b</i> [Å]	20.971(6)	7.992(3)	8.1008(7)	8.0136(16)	8.174(4)
<i>c</i> [Å]	13.735(4)	32.888(10)	11.9491(10)	14.803(4)	14.694(10)
<i>α</i> [°]	—	—	98.5504(19)	—	—
<i>β</i> [°]	—	—	108.8828(18)	111.945(4)	110.305(14)
<i>γ</i> [°]	—	—	98.007(2)	—	—
<i>V</i> [Å ³]	2237.5(12)	2682.0(17)	695.57(10)	1381.5(6)	1400.9(15)
space group	<i>Pbca</i>	<i>Pbca</i>	<i>P</i> $\bar{1}$	<i>P</i> ₂ /c	<i>P</i> ₂ /c
<i>Z</i>	8	8	2	4	4
ρ_{calcd} [g cm ^{−3}]	1.865	1.794	1.953	1.975	2.17
<i>F</i> (000)	1216	1408	388	776	848
μ (MoK α) [cm ^{−1}]	30.068	2.521	48.984	50.327	43.072
no. of reflns measured	6575	14054	6026	8205	9065
<i>R</i> _{int}	0.033	0.2862	0.072	0.039	0.032
min./max. transmissions	0.504/0.835	0.7461/1.000	0.257/0.556	0.611/0.739	0.470/0.679
independent reflns	1953	2440	2455	2759	2814
observed reflns (no. variables)	1824(128)	1526(165)	2138(164)	2579(164)	2695(164)
reflection/parameter ratio	15.26	14.79	14.97	16.82	17.16
<i>R</i> ₁ (<i>I</i> > 2.00σ(<i>I</i>))	0.0435	0.0999	0.0445	0.0483	0.0356
<i>R</i> (all reflns)	0.056	0.1347	0.0522	0.0572	0.0408
<i>wR</i> ₂ (all reflns)	0.2054	0.2692	0.1063	0.149	0.1465
GOF	1.285	0.975	1.094	1.212	1.263
flack parameter	—	—	—	—	—
max. peak in final diff. map [e Å ^{−3}]	2.18	2.198	0.77	1.50	1.41
min. peak in final diff. map [e Å ^{−3}]	−2.50	−1.651	−0.86	−1.69	−1.72

collected by using ω scans. Intensities were corrected for Lorentz, polarisation and absorption. Data for compounds **2**, **7** and **8** were collected at −148(1) °C on a Rigaku ACTOR-SM, Saturn 724 CCD area detector with graphite-monochromated MoK α radiation (λ = 0.71073 Å). The data was corrected for Lorentz, polarisation and absorption. The data for the complexes analysed was collected and processed by using CrystalClear (Rigaku).^[34] The structure was solved by using direct methods^[35] and expanded by using Fourier techniques.^[36] Non-hydrogen atoms were refined anisotropically and hydrogen atoms were refined by using the riding model. All calculations were performed by using the CrystalStructure^[37] crystallographic software package apart from refinement, which was performed by using SHELXL-97.^[38] Table 4 summarises the crystallographic data for compounds **1**, **2** and **4–8**. CCDC-663689 (**1**), -761964 (**2**), -761965 (**4**), -660322 (**5**), -761966 (**6**), -761967 (**7**) and -761968 (**8**) contain the supplementary crystallographic data for this paper. These data can be obtained free of charge from The Cambridge Crystallographic Data Centre via www.ccdc.cam.ac.uk/data_request/cif.

Computational details: Geometries were fully optimised in the gas phase at the B3LYP level^[39] by using Curtis and Binning's 962+(d) basis^[40] on Se and Br, the Stuttgart–Dresden effective core potentials along with their double zeta valence basis sets for Te and I^[41] (augmented with d-polarisation functions with exponents of 0.237 and 0.266, respectively),^[42] and 6–31+G(d) elsewhere, followed by calculation of the harmonic frequencies to confirm the minimum character of each stationary point and evaluation of Wiberg bond indices,^[32] obtained in a natural bond orbital^[43] analysis. The optimisations were started from the experimental structures available from X-ray crystallography, for which the WBIs were also calculated. The computations were performed by using the Gaussian 03 suite of programs.^[44]

Acknowledgements

Elemental analyses were performed by Sylvia Williamson and mass spectrometry was performed by Caroline Horsburgh. Calculations were performed by using the EaStCHEM Research Computing Facility maintained by Dr. H. Früchtel. The work in this project was supported by the Engineering and Physical Sciences Research Council (EPSRC). Michael Bühl wishes to thank EaStCHEM for support.

- [1] a) H. E. Katz, *J. Am. Chem. Soc.* **1985**, *107*, 1420; b) R. W. Alder, P. S. Bowman, W. R. S. Steel, D. R. Winterman, *Chem. Commun.* **1968**, 723; c) T. Costa, H. Schimdbaur, *Chem. Ber.* **1982**, *115*, 1374; d) A. Karacar, M. Freytag, H. Thönnessen, J. Omelanczuk, P. G. Jones, R. Bartsch, R. Schmutzler, *Heteroat. Chem.* **2001**, *12*, 102; e) J. Meinwald, D. Dauplaise, F. Wudl, J. J. Hauser, *J. Am. Chem. Soc.* **1977**, *99*, 255; f) R. S. Glass, S. W. Andruski, J. L. Broeker, H. Firouzabadi, L. K. Steffen, G. S. Wilson, *J. Am. Chem. Soc.* **1989**, *111*, 4036; g) T. Fujii, T. Kimura, N. Furukawa, *Tetrahedron Lett.* **1995**, *36*, 1075; h) W. Nakanishi, S. Hayashi, S. Toyota, *Chem. Commun.* **1996**, 371; i) G. P. Schiemenz, *Z. Anorg. Allg. Chem.* **2002**, *628*, 2597; j) R. J. P. Corriu, J. C. Young in *The Chemistry of Organic Silicon Compounds* (Eds.: S. Patai, Z. Rappoport), Wiley, New York, **1989**, p. 1242.
- [2] a) W. Nakanishi, S. Hayashi, *Phosphorus Sulfur Silicon Relat. Elem.* **2002**, *177*, 1833; b) W. Nakanishi, S. Hayashi, T. Uehara, *J. Phys. Chem. A* **1999**, *103*, 9906.
- [3] a) C. A. Coulson, R. Daudel, J. M. Robertson, *Proc. R. Soc. London Ser. A* **1951**, *207*, 306; b) D. W. J. Cruickshank, *Acta Crystallogr.* **1957**, *10*, 504; c) C. P. Brock, J. D. Dunitz, *Acta Crystallogr. Sect. B*

- 1982**, 38, 2218; d) J. Oddershede, S. Larsen, *J. Phys. Chem. A* **2004**, 108, 1057.
- [4] V. Balasubramanian, *Chem. Rev.* **1966**, 66, 567.
- [5] a) H. Schmidbaur, H.-J. Öller, D. L. Wilkinson, B. Huber, G. Müller, *Chem. Ber.* **1989**, 122, 31; b) H. Fujihara, N. Furukawa, *J. Mol. Struct.* **1989**, 192–215, 261; c) H. Fujihara, R. Akaishi, T. Erata, N. Furukawa, *J. Chem. Soc. Chem. Commun.* **1989**, 1789; d) J. Handal, J. G. White, R. W. Franck, Y. H. Yuh, N. L. Allinger, *J. Am. Chem. Soc.* **1977**, 99, 3345; e) J. F. Blount, F. Cozzi, J. R. Damewood, D. L. Iroff, U. Sjöstrand, K. Mislow, *J. Am. Chem. Soc.* **1980**, 102, 99; f) F. A. L. Anet, D. Donovan, U. Sjöstrand, F. Cozzi, K. Mislow, *J. Am. Chem. Soc.* **1980**, 102, 1748; g) W. D. Hounshell, F. A. L. Anet, F. Cozzi, J. R. Damewood, Jr., C. A. Johnson, U. Sjöstrand, K. Mislow, *J. Am. Chem. Soc.* **1980**, 102, 5941; h) R. Schroeck, K. Angermaier, A. Sladek, H. Schmidbaur, *Organometallics* **1994**, 13, 3399.
- [6] P. Kilian, A. M. Z. Slawin, J. D. Woollins, *Dalton Trans.* **2003**, 3876.
- [7] G. P. Schiemenz, *Z. Anorg. Allg. Chem.* **2002**, 628, 2597.
- [8] a) W. Nakanishi, S. Hayashi, *J. Org. Chem.* **2002**, 67, 38, and references therein; b) S. Hayashi, K. Yamane, W. Nakanishi, *J. Org. Chem.* **2007**, 72, 7587.
- [9] W. Nakanishi, S. Hayashi, S. Toyota, *Chem. Commun.* **1996**, 371.
- [10] W. Nakanishi, S. Hayashi, A. Sakaue, G. Ono, Y. Kawada, *J. Am. Chem. Soc.* **1998**, 120, 3635.
- [11] W. Nakanishi, S. Hayashi, T. Uehara, *Eur. J. Org. Chem.* **2001**, 3933.
- [12] a) W. Nakanishi, S. Hayashi, *J. Phys. Chem. A* **1999**, 103, 6074; b) S. Hayashi, W. Nakanishi, *J. Org. Chem.* **1999**, 64, 6688; c) W. Nakanishi, S. Hayashi, T. Arai, *Chem. Commun.* **2002**, 2416; d) S. Hayashi, H. Wada, T. Ueno, W. Nakanishi, *J. Org. Chem.* **2006**, 71, 5574; e) S. Hayashi, W. Nakanishi, *Bull. Chem. Soc. Jpn.* **2008**, 81, 1605; f) S. Hayashi, W. Nakanishi, A. Furuta, J. Drabowicz, T. Sasamori, N. Tokitoh, *New J. Chem.* **2009**, 33, 196.
- [13] a) S. M. Aucott, H. L. Milton, S. D. Robertson, A. M. Z. Slawin, G. D. Walker, J. D. Woollins, *Chem. Eur. J.* **2004**, 10, 1666–1676; b) S. M. Aucott, H. L. Milton, S. D. Robertson, A. M. Z. Slawin, J. D. Woollins, *Heteroat. Chem.* **2004**, 15, 530–542; c) S. M. Aucott, H. L. Milton, S. D. Robertson, A. M. Z. Slawin, J. D. Woollins, *Dalton Trans.* **2004**, 3347–3352; d) S. M. Aucott, P. Kilian, H. L. Milton, S. D. Robertson, A. M. Z. Slawin, J. D. Woollins, *Inorg. Chem.* **2005**, 44, 2710–2718; e) S. M. Aucott, P. Kilian, S. D. Robertson, A. M. Z. Slawin, J. D. Woollins, *Chem. Eur. J.* **2006**, 12, 895–902; f) S. M. Aucott, D. Duerden, Y. Li, A. M. Z. Slawin, J. D. Woollins, *Chem. Eur. J.* **2006**, 12, 5495–5504.
- [14] a) P. Kilian, D. Philp, A. M. Z. Slawin, J. D. Woollins, *Eur. J. Inorg. Chem.* **2003**, 249–254; b) P. Kilian, A. M. Z. Slawin, J. D. Woollins, *Chem. Eur. J.* **2003**, 9, 215–222; c) P. Kilian, A. M. Z. Slawin, J. D. Woollins, *Chem. Commun.* **2003**, 1174–1175; d) P. Kilian, H. L. Milton, A. M. Z. Slawin, J. D. Woollins, *Inorg. Chem.* **2004**, 43, 2252–2260; e) P. Kilian, A. M. Z. Slawin, J. D. Woollins, *Inorg. Chim. Acta* **2005**, 358, 1719; f) P. Kilian, A. M. Z. Slawin, J. D. Woollins, *Dalton Trans.* **2006**, 2175–2183.
- [15] F. R. Knight, A. L. Fuller, A. M. Z. Slawin, J. D. Woollins, *Dalton Trans.* **2009**, 8476–8478.
- [16] F. R. Knight, A. L. Fuller, A. M. Z. Slawin, J. D. Woollins, *Chem. Eur. J.* **2010**, 16, 7503–7516.
- [17] M. Oki, Y. Yamada, *Bull. Chem. Soc. Jpn.* **1988**, 61, 1191.
- [18] A. L. Fuller, F. R. Knight, A. M. Z. Slawin, J. D. Woollins, *Acta Crystallogr. Sect. E* **2007**, 63, o3957.
- [19] A. Toshimitsu, S. Hirao, T. Saeki, M. Asahara, K. Tamao, *Heteroat. Chem.* **2001**, 12, 392.
- [20] T. Saeki, A. Toshimitsu, K. Tamao, *Organometallics* **2003**, 22, 3299.
- [21] A. L. Fuller, F. R. Knight, A. M. Z. Slawin, J. D. Woollins, *Acta Crystallogr. Sect. E* **2007**, 63, o3855.
- [22] D. Seyferth, S. C. Vick, *J. Org. Chem.* **1977**, 141, 173.
- [23] H. O. House, D. G. Koepsell, W. J. Campbell, *J. Org. Chem.* **1972**, 37, 1003.
- [24] A. Bondi, *J. Phys. Chem.* **1964**, 68, 441.
- [25] a) N. Lozac'h, *Adv. Heterocycl. Chem.* **1971**, 13, 161; b) R. E. Rosenfield, Jr., R. Parthasarathy, J. D. Dunitz, *J. Am. Chem. Soc.* **1977**, 99, 4860; c) A. Kálmán, L. Párkányi, *Acta Crystallogr. Sect. B* **1980**, 36, 2372; d) Á. Kucsman, I. Kapovits in *Organic Sulfur Chemistry: Theoretical and Experimental Advances* (Eds.: I. G. Csizmadia, A. Mangini, F. Bernardi), Elsevier, Amsterdam, **1985**, p. 191; e) R. S. Glass, L. Adamowicz, J. L. Broeker, *J. Am. Chem. Soc.* **1991**, 113, 1065; f) F. T. Burling, B. M. Goldstein, *Acta Crystallogr. Sect. B* **1993**, 49, 738; g) Y. Nagao, T. Hirata, S. Goto, S. Sano, A. Kakehi, K. Iizuka, M. Shiro, *J. Am. Chem. Soc.* **1998**, 120, 3104; h) K. Ohkata, M. Ohsugi, K. Yamamoto, M. Ohsawa, K. Akiba, *J. Am. Chem. Soc.* **1996**, 118, 6355.
- [26] S. A. Reiter, S. D. Nogai, K. Karaghiosoff, H. Schmidbaur, *J. Am. Chem. Soc.* **2004**, 126, 15833.
- [27] P. Nagy, D. Szabó, I. Kapovits, Á. Kucsman, G. Argay, A. Kálmán, *J. Mol. Struct.* **2002**, 606, 61.
- [28] F. H. Allen, O. Kennard, D. G. Watson, L. Brammer, A. G. Orpen, R. Taylor, *J. Chem. Soc. Perkin Trans. 2* **1987**, S1.
- [29] J. G. Ángyán, R. A. Poirier, Á. Kucsman, I. G. Csizmadia, *J. Am. Chem. Soc.* **1987**, 109, 2237.
- [30] a) W. K. Musker, T. L. Wolford, *J. Am. Chem. Soc.* **1976**, 98, 3055; b) W. K. Musker, P. B. Roush, *J. Am. Chem. Soc.* **1976**, 98, 6745; c) W. K. Musker, T. L. Wolford, P. B. Roush, *J. Am. Chem. Soc.* **1978**, 100, 6416; d) W. K. Musker, *J. Am. Chem. Soc.* **1978**, 100, 6416; e) K. D. Asmus, *Acc. Chem. Res.* **1979**, 12, 436; f) W. K. Musker, T. L. Wolford, P. B. Roush, *Acc. Chem. Res.* **1980**, 13, 200; g) T. G. Brown, A. S. Hirschon, W. K. Musker, *J. Phys. Chem.* **1981**, 85, 3767.
- [31] a) R. S. Mulliken, *J. Am. Chem. Soc.* **1950**, 72, 600; b) R. S. Mulliken, *J. Am. Chem. Soc.* **1952**, 74, 811; c) S. P. McGlynn, *Chem. Soc. Rev.* **1958**, 13, 1113.
- [32] K. B. Wiberg, *Tetrahedron* **1968**, 24, 1083.
- [33] For 1,6-dibromo-2-phenyl-1,2-diselenanaphthylene (two molecules in the unit cell with Se–Se distances of 2.516 and 2.542 Å), see: E. Horn, T. Nakahodo, N. Fukurawa, *Z. Kristallogr. New Cryst. Struct.* **2000**, 215, 23.
- [34] CrystalClear v.1.6, Rigaku Corporation, **1999**; CrystalClear Software User's Guide, Molecular Structure Corporation, **2000**; J. W. P. Pflugrath, *Acta Crystallogr. Sect. D* **1999**, 55, 1718.
- [35] A. Altomare, M. Burla, M. Camalli, G. Casciaro, C. Giacovazzo, A. Guagliardi, A. Moliterni, G. Polidori, R. Spagna, *J. Appl. Crystallogr.* **1999**, 32, 115.
- [36] P. T. Beurskens, G. Admiraal, G. Beurskens, W. P. Bosman, R. de Gelder, R. Israel, J. M. M. Smits, The DIRDIF-99 program system, Technical Report of the Crystallography Laboratory, University of Nijmegen, Nijmegen, **1999**.
- [37] CrystalStructure v. 3.8.1, Crystal Structure Analysis Package, Rigaku and Rigaku/MS, Rigaku Americas, **2000–2006**.
- [38] G. M. Sheldrick, *Acta Crystallogr. Sect. A* **2008**, 64, 112.
- [39] a) A. D. Becke, *J. Chem. Phys.* **1993**, 98, 5648; b) C. Lee, W. Yang, R. G. Parr, *Phys. Rev. B* **1988**, 37, 785.
- [40] R. C. Binning, L. A. Curtiss, *J. Comput. Chem.* **1990**, 11, 1206.
- [41] a) P. Schwerdtfeger, M. Dolg, W. H. E. Schwarz, G. A. Bowmaker, P. D. W. Boyd, *J. Chem. Phys.* **1989**, 91, 1762; b) A. Bergner, M. Dolg, W. Kuechle, H. Stoll, H. Preuss, *Mol. Phys.* **1993**, 80, 1431; c) the valence basis by Kaupp et al. (including diffuse functions) was employed for I, see: M. Kaupp, P. von R. Schleyer, H. Stoll, H. Preuss, *J. Am. Chem. Soc.* **1991**, 113, 6012.
- [42] S. Huzinaga, J. Anzelm, M. Klobukowski, E. Radzio-Andzelm, Y. Sakai, H. Tatewaki in *Gaussian Basis Sets for Molecular Calculations*, Elsevier, Amsterdam, **1984**.
- [43] A. E. Reed, L. A. Curtiss, F. Weinhold, *Chem. Rev.* **1988**, 88, 899.
- [44] Gaussian 03, Revision E 01, M. J. Frisch, G. W. Trucks, H. B. Schlegel, G. E. Scuseria, M. A. Robb, J. R. Cheeseman, J. A. Montgomery, Jr., T. Vreven, K. N. Kudin, J. C. Burant, J. M. Millam, S. S. Iyengar, J. Tomasi, V. Barone, B. Mennucci, M. Cossi, G. Scalmani, N. Rega, G. A. Petersson, H. Nakatsuji, M. Hada, M. Ehara, K. Toyota, R. Fukuda, J. Hasegawa, M. Ishida, T. Nakajima, Y. Honda, O. Kitao, H. Nakai, M. Klene, X. Li, J. E. Knox, H. P. Hratchian, J. B. Cross, V. Bakken, C. Adamo, J. Jaramillo, R. Gomperts, R. E. Stratmann, O. Yazyev, A. J. Austin, R. Cammi, C. Pomelli, J. W.

Ochterski, P. Y. Ayala, K. Morokuma, G. A. Voth, P. Salvador, J. J. Dannenberg, V. G. Zakrzewski, S. Dapprich, A. D. Daniels, M. C. Strain, O. Farkas, D. K. Malick, A. D. Rabuck, K. Raghavachari, J. B. Foresman, J. V. Ortiz, Q. Cui, A. G. Baboul, S. Clifford, J. Cioslowski, B. B. Stefanov, G. Liu, A. Liashenko, P. Piskorz, I. Komaromi, R. L. Martin, D. J. Fox, T. Keith, M. A. Al-Laham, C. Y. Peng,

A. Nanayakkara, M. Challacombe, P. M. W. Gill, B. Johnson, W. Chen, M. W. Wong, C. Gonzalez, J. A. Pople, Gaussian, Inc., Wallingford CT, **2004**.

Received: February 18, 2010
Published online: May 19, 2010